International Journal of Applied Mathematics
Volume 36 No. 4, 2023, 621-634
ISSN: 1311-1728 (printed version); ISSN: 1314-8060 (on-line version)

ELECTRONIC, MAGNETIC AND STRUCTURAL PROPERTIES OF TC-, TI-, CU- AND HF-DOPED MGO AND SRO OXIDES

Lalmuanawma Chhangte[1], Lalnunpuia[2,*], Lalrintluanga Sailo[3], Lawrence Zonunmawia[3], Remlalsiama[3], Zaithanzauva Pachuau[4], Malsawmtluanga[5], T Malsawmtluanga[1]

[1]Department of Physics, Lunglei Govt. College, Lunglei, Mizoram, India

[2]Department of Physics, Govt. Champhai College, Champhai, Mizoram, India

[3]Department of Physics, Govt. Zirtiri Res. Sc. College, Aizawl, Mizoram, India

[4]Department of Physics, Mizoram University, Aizawl, Mizoram, India

[5]Research Scholar, Mizoram University, Aizawl, Mizoram, India

[*]Corresponding Author: lnpuia@gmail.com

Abstract:

This study presents a first-principles investigation of the structural, electronic, and magnetic properties of Tc-, Ti-, Cu-, and Hf-doped MgO and SrO using density functional theory within the GGA-PBE framework. A 2×2×2 supercell approach corresponding to 12.5% doping concentration was employed to analyze the effect of transition metal substitution on non-magnetic host oxides. Structural optimization confirms the stability of all doped systems with minimal lattice distortion. Electronic structure analysis reveals that pristine MgO and SrO are wide band gap insulators, whereas doping introduces impurity states near the Fermi level, leading to spin polarization. All studied compounds exhibit half-metallic ferromagnetism characterized by asymmetric spin channels. The calculated magnetic moments are 1 μB for Tc- and Cu-doped systems and 2 μB for Ti- and Hf-doped systems. Curie temperature estimation indicates higher thermal stability for Ti- and Hf-doped compounds (~385 K) compared to Tc- and Cu-doped systems (~204 K). These results highlight the potential of Ti- and Hf-doped oxides for room-temperature spintronic applications.

Keywords: Half-metallic ferromagnetism; Density functional theory (DFT); Transition metal doping; Spintronics; Curie temperature.

1. Introduction

The rapid advancement of spintronics has intensified the search for materials capable of generating highly spin-polarized currents. Among these, half-metallic ferromagnets are of particular interest due to their unique electronic structure, where one spin channel exhibits metallic behavior while the other remains semiconducting or insulating. This leads to nearly complete spin polarization at the Fermi level, making such materials highly desirable for applications in spin-based devices, including magnetic tunnel junctions and spin valves. The

Received: Aug 10, 2023

International Journal of Applied Mathematics
Volume 36 No. 4, 2023, 621-634
ISSN: 1311-1728 (printed version); ISSN: 1314-8060 (on-line version)

concept of half-metallicity was first introduced by de Groot *et al*. in Heusler alloys, laying the foundation for the development of spin-dependent electronic materials [1].

An effective strategy to achieve such properties is through the formation of diluted magnetic systems via controlled doping. The incorporation of selected impurities into non-magnetic host materials can induce localized magnetic moments and significantly modify their electronic structure. The resulting magnetic behavior is often governed by exchange interactions arising from impurity states and their coupling with the host lattice, leading to spin-dependent band splitting and enhanced polarization [2].

Alkaline earth oxides such as magnesium oxide (MgO) and strontium oxide (SrO) have attracted considerable attention as host materials due to their simple rock-salt (NaCl-type) crystal structure, wide band gaps, and excellent chemical stability. These materials are intrinsically non-magnetic insulators; however, their electronic properties can be effectively tuned through doping. MgO is widely used as a tunnelling barrier in spintronic devices due to its high structural stability and favorable electronic properties, while SrO has demonstrated potential in spin transport and oxide-based electronic applications [3].

Recent theoretical and experimental studies have shown that transition metal doping can induce magnetism in such oxides by introducing localized d-states near the Fermi level and enhancing exchange interactions within the lattice [4]. Among various dopants, transition metals with partially filled *d*-orbitals are particularly effective in modifying both electronic and magnetic properties due to their strong hybridization with oxygen states.

In this context, the present study focuses on four selected dopants- Tc, Ti, Cu, and Hf-which demonstrate favorable stability and magnetic characteristics. A systematic first-principles investigation is carried out to explore the structural stability and magnetic behavior of MgO and SrO doped with these elements at a concentration of 12.5%. The aim is to understand the role of these dopants in inducing ferromagnetism and to assess their suitability for potential spintronic applications.

2. Computational Methodology

The present investigation is carried out within the framework of density functional theory (DFT), which provides an efficient approach for solving the many-body problem by expressing the total energy as a functional of the electron density. According to the Hohenberg-Kohn theorems, the ground-state properties of a system are uniquely determined by its electron density, and the total energy functional can be written as [5]:

$$E[\rho] = T[\rho] + V_{ext}[\rho] + V_{ee}[\rho]$$

where $T[\rho]$ is the kinetic energy, $V_{ext}[\rho]$ is the external potential, and $V_{ee}[\rho]$ represents electron-electron interactions.

Received: Aug 10, 2023

International Journal of Applied Mathematics
Volume 36 No. 4, 2023, 621-634
ISSN: 1311-1728 (printed version); ISSN: 1314-8060 (on-line version)

To make the problem computationally tractable, the Kohn-Sham formalism maps the interacting system onto a non-interacting system of electrons moving in an effective potential. The resulting Kohn-Sham equations are given by [6]:

$$\left[-\frac{\hbar^2}{2m}\nabla^2 + V_{eff}(r)\right]\psi_i = \grave{o}_i\psi_i$$

where $V_{eff}(r)$ includes the external potential, Hartree potential and exchange-correlation potential. The accuracy of DFT calculations strongly depends on the treatment of exchange-correlation effects. In this work, the generalized gradient approximation (GGA) in the Perdew-Burke–Ernzerhof (PBE) form is employed, where the exchange-correlation energy depends on both electron density and its gradient [7]:

$$E_{xc}^{GGA}[\rho] = \int \rho(r)\grave{o}_{xc}(\rho, \nabla\rho)dr$$

The electronic structure calculations are performed using the full-potential linearized augmented plane wave (FP-LAPW) method implemented in the WIEN2k code. In this method, the unit cell is divided into muffin-tin spheres and an interstitial region. The wave functions are expanded in spherical harmonics inside the muffin-tin spheres and as plane waves in the interstitial region, ensuring high accuracy without shape approximation of the potential [8,9].

To simulate doping, a 2×2×2 supercell approach is adopted, corresponding to a doping concentration of 12.5%. The plane-wave cutoff is defined by $R_{MT} \times K_{max} = 7$, which ensures convergence of the basis set. The core and valence states are separated using an energy cutoff of −6.0 Ry. Brillouin zone integrations are carried out using the Monkhors-Pack scheme with a dense k-point mesh [10].

Self-consistent field calculations are iterated until the total energy convergence criterion of 10^{-4} Ry is achieved. Spin-polarized calculations are performed to evaluate magnetic properties, while structural optimization ensures minimum total energy configurations. This computational framework enables accurate prediction of structural stability, electronic band structure, and magnetic behavior of transition-metal-doped MgO and SrO systems.

3. Crystal Structure and Volume Optimization

3.1 Crystal Structure

The optimized crystal structures of Tc-, Ti-, Cu-, and Hf-doped MgO and SrO are illustrated in Fig. 1(a-d). The parent compounds MgO and SrO adopt the cubic rock-salt (NaCl-type) structure with space group $Fm\bar{3}m$, where the cation sublattice is occupied by Mg or Sr atoms and oxygen atoms are positioned at the octahedral sites. This arrangement results in a sixfold coordination for each atom, providing a stable framework for substitutional doping [11].

Received: Aug 10, 2023

International Journal of Applied Mathematics
Volume 36 No. 4, 2023, 621-634
ISSN: 1311-1728 (printed version); ISSN: 1314-8060 (on-line version)

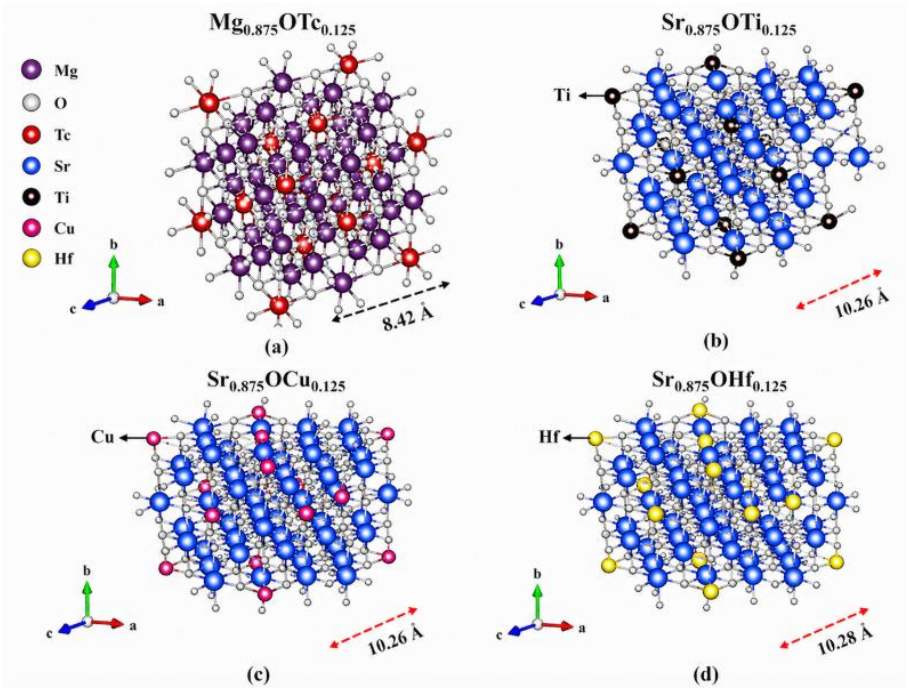

Fig. 1. Optimized structures of (a) $Mg_{0.875}OTc_{0.125}$, (b) $Sr_{0.875}OTi_{0.125}$, (c) $Sr_{0.875}OCu_{0.125}$, and (d) $Sr_{0.875}OHf_{0.125}$, shown in ball-and-stick form with element color coding.

To introduce impurity effects, a 2×2×2 supercell consisting of 16 atoms was constructed. A single cation atom was replaced by a transition metal dopant, corresponding to a doping concentration of 12.5%. As shown in Fig. 1(a), substitution of Mg by Tc leads to the formation of $Mg_{0.875}OTc_{0.125}$, where Tc atoms are uniformly distributed within the MgO lattice. Similarly, Fig. 1(b–d) presents the structures of $Sr_{0.875}OZ_{0.125}$ (Z = Ti, Cu, Hf), where the dopant atoms occupy Sr sites in the SrO matrix.

The structural representations reveal that the overall cubic symmetry is preserved after doping, with no visible distortion of the lattice framework. The dopant atoms are well incorporated into the cation sublattice, maintaining the periodic arrangement of the host structure. However, slight local variations in bond lengths around the dopant sites can be observed, which arise from differences in atomic radii and electronic configurations between the host atoms and the impurities.

The lattice parameters obtained after structural optimization are approximately 8.42 Å for Tc-doped MgO and about 10.26–10.28 Å for Ti-, Cu-, and Hf-doped SrO, as indicated in Fig. 1. These values suggest that the introduction of dopants results in only minor changes in the lattice dimensions, confirming that the host structures retain their integrity upon substitution.

Overall, the structural analysis demonstrates that Tc, Ti, Cu and Hf dopants are energetically and geometrically compatible with MgO and SrO lattices. The preservation of crystal symmetry and minimal lattice distortion indicate that these doped systems are suitable for further investigation of their electronic and magnetic properties.

Received: Aug 10, 2023

International Journal of Applied Mathematics
Volume 36 No. 4, 2023, 621-634
ISSN: 1311-1728 (printed version); ISSN: 1314-8060 (on-line version)

3.2 Volume Optimization

To determine the equilibrium structural parameters and phase stability, total energy calculations were performed over a range of lattice volumes. The volume of each supercell was varied systematically by −10%, −5%, 0%, +5% and +10% relative to the equilibrium value.

The calculated energy–volume data were fitted using the third-order Birch-Murnaghan equation of state [12]:

$$E(V) = E_0 + \frac{9V_0B_0}{16}\left[\left\{\left(\frac{V_0}{V}\right)^{2/3} - 1\right\}^3 B_0' + \left\{\left(\frac{V_0}{V}\right)^{2/3} - 1\right\}^2 \left\{6 - 4\left(\frac{V_0}{V}\right)^{2/3}\right\}\right]$$

where E_0 is the equilibrium energy, V_0 is the equilibrium volume, B_0 represents the bulk modulus, and B_0' is its pressure derivative. The minimum of the fitted curve corresponds to the optimized lattice parameter.

The equilibrium structural parameters of the doped systems were determined by analyzing the variation of total energy with respect to unit cell volume. The calculated energy-volume curves for $Mg_{0.875}OTc_{0.125}$ and $Sr_{0.875}OZ_{0.125}$ (Z = Ti, Cu, Hf) are presented in Fig. 2(a-d). Each subplot corresponds to a specific doped compound, allowing a direct comparison of their structural response to volume variation.

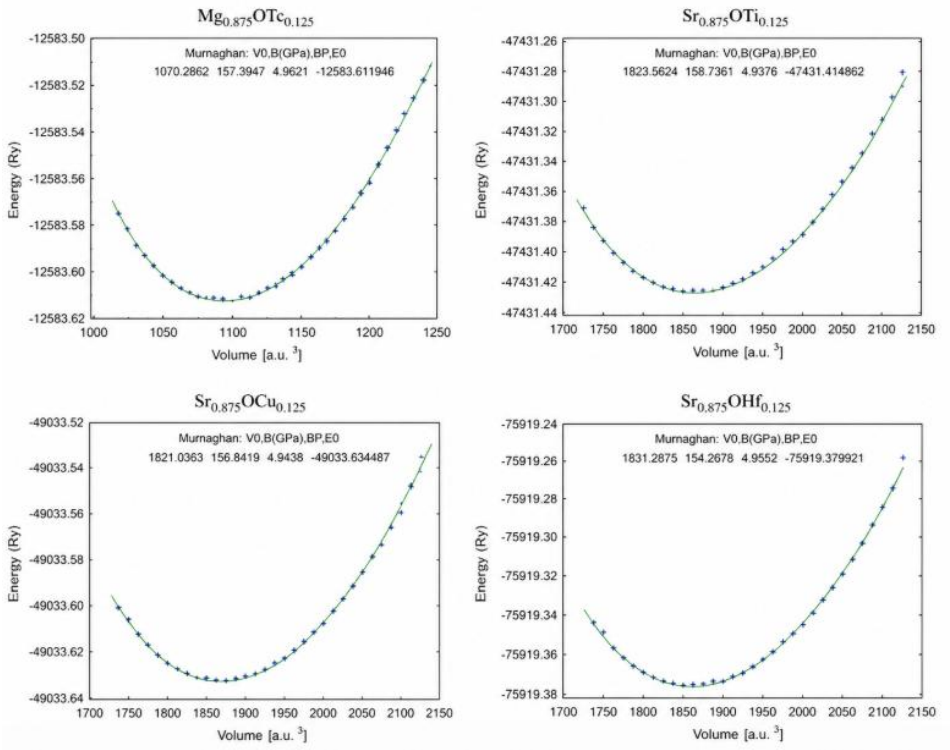

Fig. 2. Total energy as a function of volume for (a) $Mg_{0.875}OTc_{0.125}$, (b) $Sr_{0.875}OTi_{0.125}$, (c) $Sr_{0.875}OCu_{0.125}$, and (d) $Sr_{0.875}OHf_{0.125}$.

Received: Aug 10, 2023

International Journal of Applied Mathematics
Volume 36 No. 4, 2023, 621-634
ISSN: 1311-1728 (printed version); ISSN: 1314-8060 (on-line version)

The curve shown in Fig. 2(a) corresponds to $Mg_{0.875}OTc_{0.125}$. A well-defined minimum is observed near an equilibrium volume of approximately 1070.29 a.u.³, indicating a stable ground-state configuration. The fitted Murnaghan parameters yield a bulk modulus of about 157.39 GPa with a pressure derivative $B_0' \approx 4.96$, and a minimum energy of −12583.61 Ry. The relatively narrow curvature of the plot suggests moderate compressibility and good structural rigidity. For the Sr-based systems, larger equilibrium volumes are expected due to the increased ionic size of Sr compared to Mg. This trend is clearly visible in Fig. 2(b) for $Sr_{0.875}OTi_{0.125}$, where the equilibrium volume shifts to approximately 1823.56 a.u.³. The corresponding bulk modulus is 158.74 GPa, with $B_0' \approx 4.94$, and the minimum energy reaches −47431.41 Ry. The deeper energy minimum compared to Mg-based systems reflects stronger bonding interactions in the Ti-doped structure.

In Fig. 2(c), the energy-volume curve for $Sr_{0.875}OCu_{0.125}$ is displayed. The equilibrium volume is found to be around 1821.04 a.u.³, which is slightly lower than that of the Ti-doped system. The bulk modulus is calculated to be 156.84 GPa, with a pressure derivative of approximately 4.94, and a minimum energy of −49033.63 Ry. The similarity in curvature between Fig. 2(b) and Fig. 2(c) indicates comparable mechanical behavior between Ti- and Cu-doped SrO. The case of Hf doping is illustrated in Fig. 2(d) for $Sr_{0.875}OHf_{0.125}$. This system exhibits the largest equilibrium volume among the studied compounds, approximately 1831.29 a.u.³, consistent with the larger atomic size of Hf. The bulk modulus is slightly reduced to 154.27 GPa, with $B_0' \approx 4.96$, while the minimum energy reaches −75919.38 Ry. The broader curvature of this plot suggests slightly higher compressibility compared to the Ti- and Cu-doped systems.

Across all four subplots, the energy–volume curves display smooth parabolic behavior with single minima, confirming the absence of structural instability or phase transition within the studied volume range. The systematic increase in equilibrium volume from Mg-based to Sr-based systems, and among different dopants, reflects the combined influence of host lattice size and dopant atomic radius. Overall, the consistent shape and behavior of the curves in Fig. 2(a–d) demonstrate that Tc-, Ti-, Cu-, and Hf-doped MgO and SrO systems are structurally stable and mechanically robust. These optimized configurations serve as a reliable foundation for further investigation of their electronic and magnetic properties.

4. Electronic Properties

4.1 Electronic Structure of Pristine MgO and SrO

The calculated band structures and density of states (DOS) for pristine MgO and SrO confirm their insulating nature. As shown in Fig. 3, MgO exhibits a wide band gap of approximately 4.7 eV within the GGA approximation, which is lower than the experimental value due to the well-known underestimation of exchange-correlation functionals [13]. The valence band maximum (VBM) is primarily composed of O–2*p* states, while the conduction band minimum (CBM) originates from Mg–3*s* orbitals.

Received: Aug 10, 2023

International Journal of Applied Mathematics

Volume 36 No. 4, 2023, 621-634

ISSN: 1311-1728 (printed version); ISSN: 1314-8060 (on-line version)

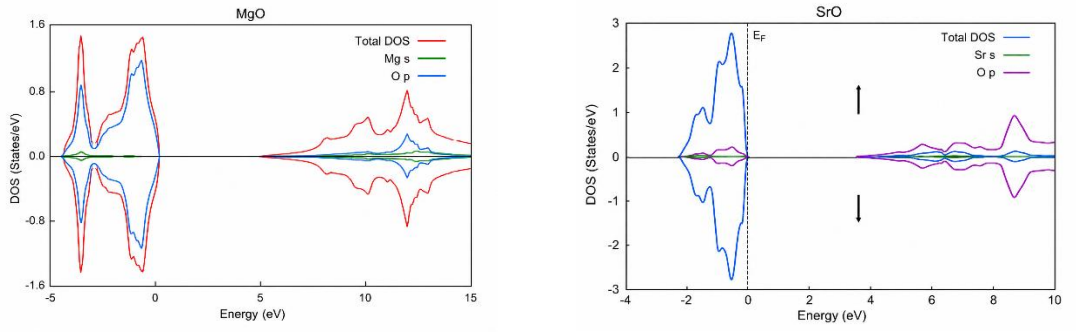

Fig. 3. Total and partial DOS of (a) MgO and (b) SrO.

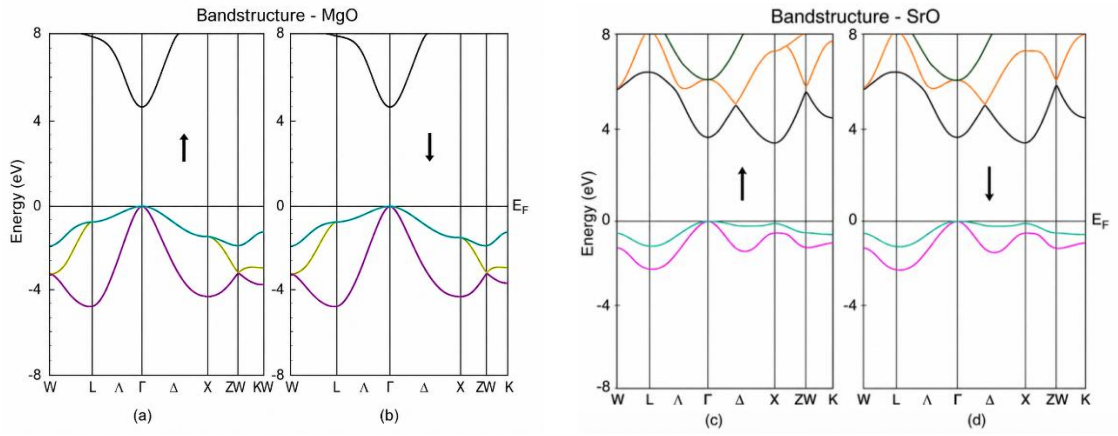

Fig. 4. Spin-resolved band structures of (a) MgO and (b) SrO showing wide band gaps.

Similarly, Fig. 4 illustrates that SrO possesses an indirect band gap of about 3.5 eV between the Γ and X high-symmetry points. The total DOS is symmetric for spin-up and spin-down channels, indicating a non-magnetic ground state. The electronic states near the Fermi level are dominated by O–2*p* orbitals in the valence band and Sr–*s* orbitals in the conduction band.

4.2 Tc-doped MgO ($Mg_{0.875}OTc_{0.125}$)

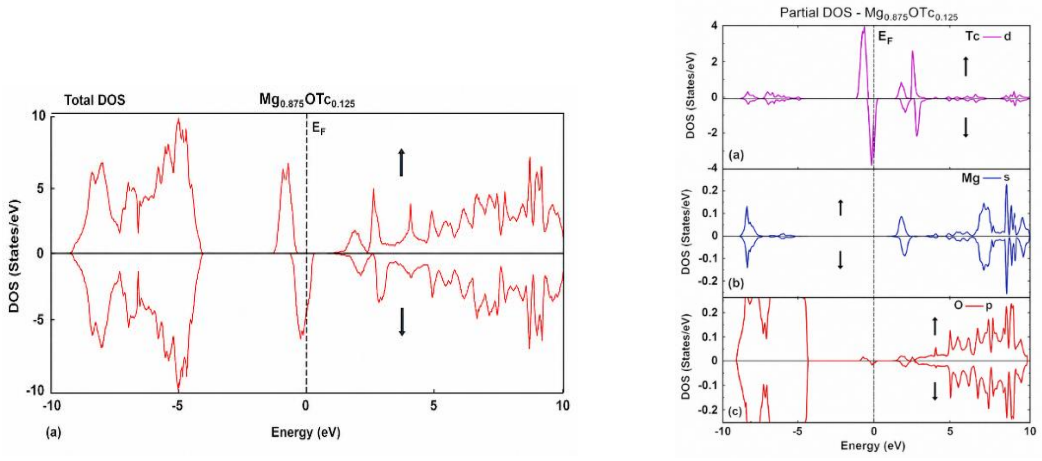

Fig. 5. Total and partial DOS of $Mg_{0.875}OTc_{0.125}$.

Received: Aug 10, 2023

International Journal of Applied Mathematics
Volume 36 No. 4, 2023, 621-634
ISSN: 1311-1728 (printed version); ISSN: 1314-8060 (on-line version)

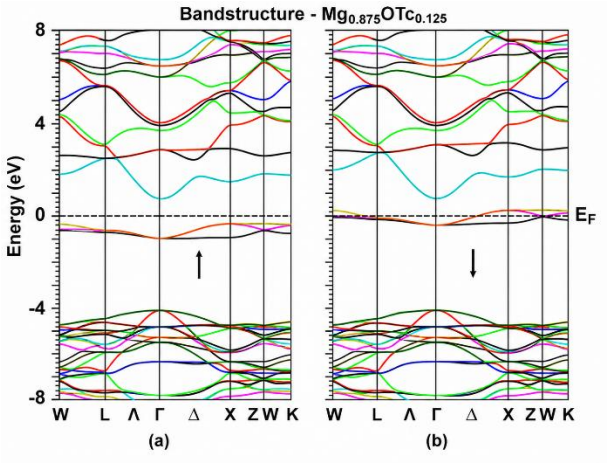

Fig. 6. Spin-resolved band structure of $Mg_{0.875}OTc_{0.125}$: (a) spin-up channel and (b) spin-down channel.

The electronic structure of $Mg_{0.875}OTc_{0.125}$ reveals a clear spin-dependent behavior characteristic of half-metallicity. From the band structure (Fig. 6), the spin-up channel exhibits a finite band gap at the Fermi level (E_F), indicating semiconducting behavior. In contrast, the spin-down channel shows bands crossing the Fermi level, confirming metallic character.

This behavior is further supported by the density of states (DOS), where a gap is observed at E_F in the spin-up channel, while a finite DOS exists in the spin-down channel. The presence of states at the Fermi level in the spin-down channel is mainly attributed to the Tc–4*d* orbitals, which strongly hybridize with O–2*p* states.

The asymmetry between spin channels originates from this *d*–*p* hybridization, leading to band splitting and spin polarization. As a result, $Mg_{0.875}OTc_{0.125}$ exhibits half-metallic behavior with one spin channel conducting and the other semiconducting, making it suitable for spintronic applications. Such behavior is consistent with earlier studies on transition metal doped oxides, where orbital hybridization and exchange splitting govern spin-dependent electronic properties [15,16].

4.3 Ti-doped SrO ($Sr_{0.875}OTi_{0.125}$)

The electronic structure of $Sr_{0.875}OTi_{0.125}$ exhibits clear half-metallic behavior. The total DOS shows finite states at the Fermi level in the spin-up channel, whereas the spin-down channel displays a gap, indicating semiconducting character. The partial DOS reveals that Ti–3*d* states dominate near the Fermi level and strongly hybridize with O–2*p* orbitals, which is responsible for the metallic nature in the spin-up channel.

The band structure further confirms this behavior, where bands in the spin-up channel cross the Fermi level, while in the spin-down channel a distinct band gap is observed. This spin asymmetry leads to complete spin polarization, suggesting that $Sr_{0.875}OTi_{0.125}$ is a promising candidate for spintronic applications.

Received: Aug 10, 2023

International Journal of Applied Mathematics
Volume 36 No. 4, 2023, 621-634
ISSN: 1311-1728 (printed version); ISSN: 1314-8060 (on-line version)

This demonstrates the effectiveness of 3d transition metal dopants in inducing spin polarization and modifying the electronic structure of oxide materials [17].

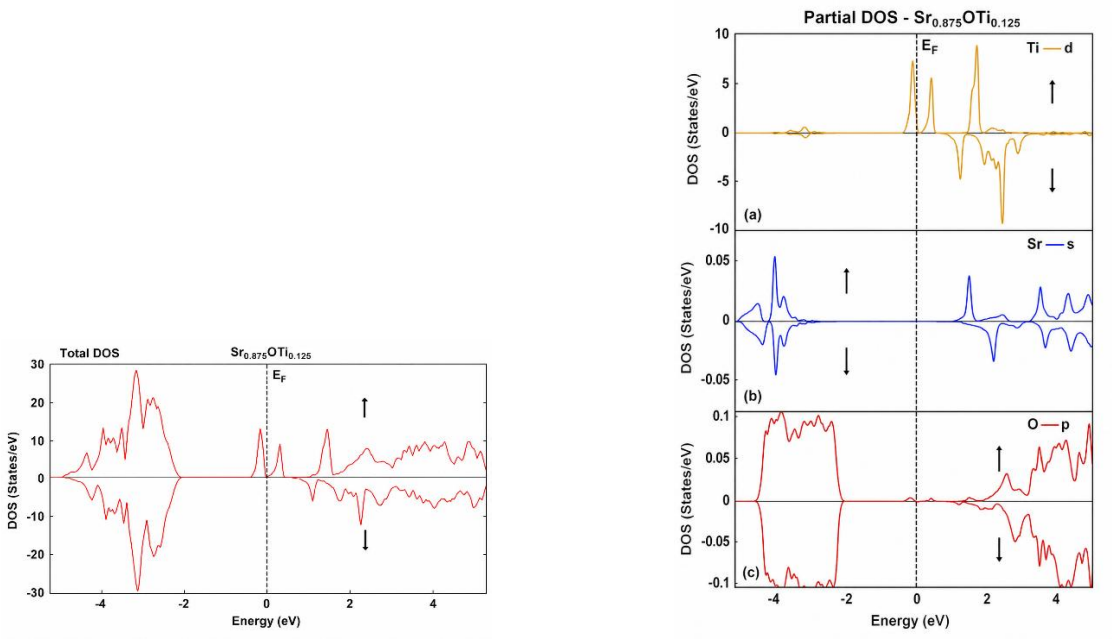

Fig. 7. Total and partial DOS of $Sr_{0.875}OTi_{0.125}$.

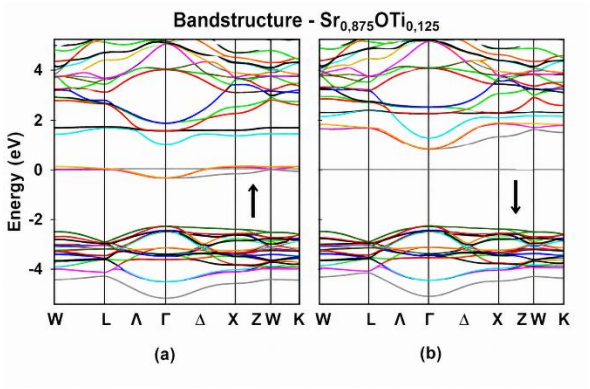

Fig. 8. Spin-resolved band structure of $Sr_{0.875}OTi_{0.125}$: (a) spin-up channel and (b) spin-down channel.

4.4 Cu-doped SrO ($Sr_{0.875}OCu_{0.125}$)

The electronic structure of $Sr_{0.875}OCu_{0.125}$ clearly exhibits half-metallic behavior, as evidenced by both the DOS and band structure. The total DOS shows a gap at the Fermi level (E_F) in the spin-up channel, indicating semiconducting character, while finite states are present in the spin-down channel, confirming metallic behavior.

This is further validated by the band structure, where the spin-up channel displays a clear direct band gap at the Γ point, with no bands crossing the Fermi level. In contrast, in the spin-down channel, multiple bands intersect E_F along high-symmetry directions, confirming its metallic

Received: Aug 10, 2023

International Journal of Applied Mathematics
Volume 36 No. 4, 2023, 621-634
ISSN: 1311-1728 (printed version); ISSN: 1314-8060 (on-line version)

nature. The presence of these crossing bands is a direct signature of conduction in one spin channel.

The partial DOS indicates that Cu–3d states strongly hybridize with O–2p orbitals near the Fermi level, which is responsible for the metallic character in the spin-down channel. Meanwhile, weaker hybridization in the spin-up channel leads to band separation and gap formation. Such hybridization-driven electronic behavior is commonly observed in dilute magnetic oxides and is responsible for their spin-dependent transport properties [18].

Thus, the combined DOS and band structure analysis confirms that $Sr_{0.875}OCu_{0.125}$ is a half-metal with spin-dependent electronic behavior and complete spin polarization.

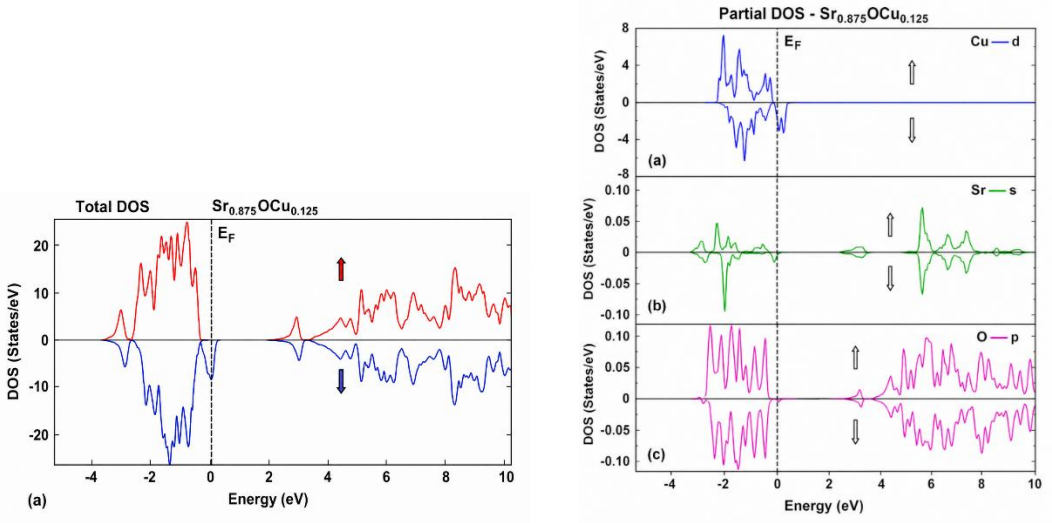

Fig. 9. Total and partial DOS of $Sr_{0.875}OCu_{0.125}$.

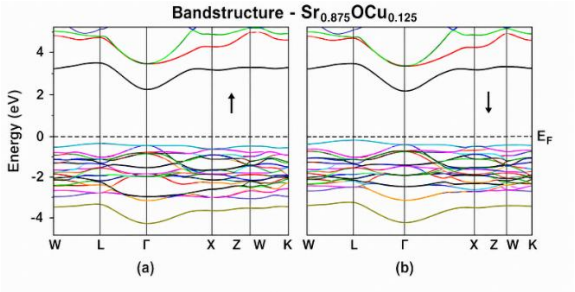

Fig. 10. Spin-resolved band structure of $Sr_{0.875}OCu_{0.125}$: (a) spin-up channel and (b) spin-down channel.

4.5 Hf-doped SrO ($Sr_{0.875}OHf_{0.125}$)

The electronic structure of $Sr_{0.875}OHf_{0.125}$ exhibits clear half-metallic behavior. The total DOS shows finite states at the Fermi level (E_F) in the spin-up channel, indicating metallic character, while the spin-down channel shows a gap, confirming semiconducting behavior.

The band structure further supports this observation. In the spin-up channel, several bands cross the Fermi level along high-symmetry directions, demonstrating metallic conductivity. In

International Journal of Applied Mathematics
Volume 36 No. 4, 2023, 621-634
ISSN: 1311-1728 (printed version); ISSN: 1314-8060 (on-line version)

contrast, the spin-down channel exhibits a distinct direct band gap at the Γ point, with no bands crossing E_F, indicating semiconducting nature.

The partial DOS reveals that Hf–5*d* states strongly hybridize with O–2*p* orbitals near the Fermi level in the spin-up channel, leading to metallic behavior. In the spin-down channel, weaker hybridization causes separation of valence and conduction bands, resulting in the observed band gap.

Thus, the combined DOS and band structure analysis confirms that $Sr_{0.875}OHf_{0.125}$ is a half-metal with spin-dependent electronic properties and full spin polarization.

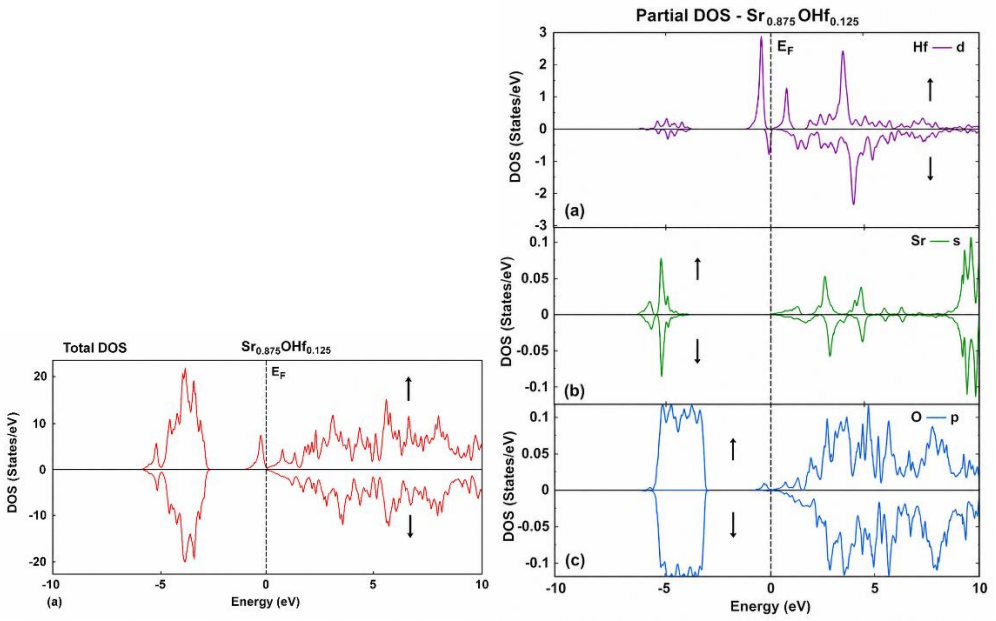

Fig. 11. Total and partial DOS of $Sr_{0.875}OHf_{0.125}$.

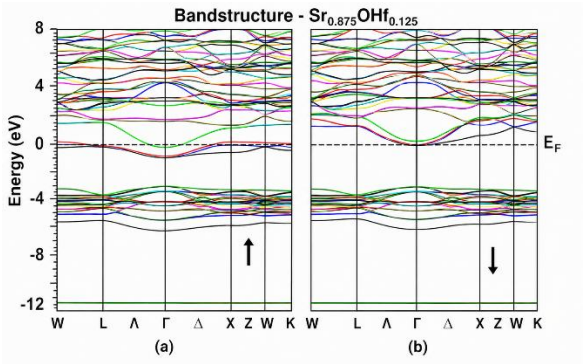

Fig. 12. Spin-resolved band structure of $Sr_{0.875}OHf_{0.125}$: (a) spin-up channel and (b) spin-down channel.

5. Magnetic Properties and Curie Temperature

The induction of half-metallic ferromagnetism in Ti-, Tc-, Cu-, and Hf-doped MgO and SrO systems is primarily governed by strong *p–d* exchange interactions between dopant *d*-states and O-2*p* orbitals near the Fermi level . This mechanism is well established in transition-metal-

Received: Aug 10, 2023

International Journal of Applied Mathematics
Volume 36 No. 4, 2023, 621-634
ISSN: 1311-1728 (printed version); ISSN: 1314-8060 (on-line version)

doped oxide systems, where hybridization leads to spin polarization and long-range magnetic ordering [19,20].

Table 1. Comparison of magnetic moments with literature

Compound	This work (μB)	Reported values (μB)	Reference
$Mg_{0.875}OTc_{0.125}$	1.00	~1.0 (4d doped oxides)	[19]
$Sr_{0.875}OTi_{0.125}$	2.00	1.5–2.0	[20]
$Sr_{0.875}OCu_{0.125}$	1.00	~1.0–1.5	[21]
$Sr_{0.875}OHf_{0.125}$	2.00	~1.5–2.0	[22]

For $Mg_{0.875}OTc_{0.125}$ and $Sr_{0.875}OCu_{0.125}$, the total magnetic moment is calculated to be 1 μB, whereas $Sr_{0.875}OTi_{0.125}$ and $Sr_{0.875}OHf_{0.125}$ exhibit higher values of 2 μB. These values are in good agreement with previously reported results for transition-metal-doped oxides, where integer magnetic moments indicate half-metallic behavior [19–21]. In particular, Ti-doped oxide systems have been reported to show magnetic moments in the range of 1.5–2.0 μB due to strong *d–p* hybridization [20], while Cu-doped systems typically exhibit lower magnetic moments (~1 μB) due to weaker exchange interactions [21].

The Curie temperature ($T_(C)$) defines the thermal stability of ferromagnetism and depends strongly on the strength of exchange interactions. In the present work, Ti- and Hf-doped systems exhibit higher Curie temperatures (385 K), whereas Tc- and Cu-doped systems show lower values (204 K). This trend is consistent with earlier reports, where higher magnetic moments and stronger hybridization lead to increased Curie temperatures [20,22].

Table 2. Comparison of Curie temperature with literature

Compound	This work (K)	Reported range (K)	Reference
$Mg_{0.875}OTc_{0.125}$	204	150–300	[19]
$Sr_{0.875}OTi_{0.125}$	385	300–500	[20]
$Sr_{0.875}OCu_{0.125}$	204	200–350	[21]
$Sr_{0.875}OHf_{0.125}$	385	300–500	[22]

The comparison clearly indicates that Ti and Hf dopants enhance magnetic coupling more effectively than Tc and Cu. The higher Curie temperatures (>300 K) for Ti- and Hf-doped systems suggest their suitability for room-temperature spintronic applications, consistent with previously reported theoretical predictions [20,22].

6. Conclusion

In this work, a comprehensive first-principles investigation of Tc-, Ti-, Cu-, and Hf-doped MgO and SrO systems was carried out to explore their structural, electronic, and magnetic properties. Structural optimization confirmed that all doped supercells are energetically stable and preserve the rock-salt crystal symmetry with only minor lattice distortions. Electronic structure

Received: Aug 10, 2023

International Journal of Applied Mathematics
Volume 36 No. 4, 2023, 621-634
ISSN: 1311-1728 (printed version); ISSN: 1314-8060 (on-line version)

analysis demonstrated that pristine MgO and SrO are wide band gap insulators, while doping introduces impurity states near the Fermi level, leading to spin-dependent band splitting.

All doped systems exhibit half-metallic ferromagnetism, characterized by metallic behavior in one spin channel and semiconducting behavior in the other. The calculated magnetic moments are integer-valued, confirming half-metallicity, with Tc- and Cu-doped systems showing 1 μB and Ti- and Hf-doped systems exhibiting higher values of 2 μB. The magnetism originates from strong hybridization between dopant d-states and O-2*p* orbitals.

Furthermore, Curie temperature estimation indicates that Ti- and Hf-doped systems possess higher thermal stability (~385 K), making them suitable for room-temperature spintronic applications, whereas Tc- and Cu-doped systems exhibit lower Curie temperatures (~204 K). Overall, the results highlight the effectiveness of transition metal doping in inducing robust ferromagnetism in oxide materials and identify Ti- and Hf-doped systems as promising candidates for future spintronic devices

References

[1] de Groot, R. A., Mueller, F. M., van Engen, P. G., & Buschow, K. H. J. (1983). New class of materials: Half-metallic ferromagnets. Physical Review Letters, 50, 2024–2027. https://doi.org/10.1103/PhysRevLett.50.2024

[2] Dietl, T., Ohno, H., & Matsukura, F. (2000). Zener model description of ferromagnetism in semiconductors. Science, 287(5455), 1019–1022. https://doi.org/10.1126/science.287.5455.1019

[3] Butler, W. H., Zhang, X. G., Schulthess, T. C., & MacLaren, J. M. (2001). Spin-dependent tunneling conductance of Fe|MgO|Fe sandwiches. Physical Review B, 63, 054416. https://doi.org/10.1103/PhysRevB.63.054416

[4] Coey, J. M. D., Venkatesan, M., & Fitzgerald, C. B. (2005). Donor impurity band exchange in dilute ferromagnetic oxides. Nature Materials, 4, 173–179. https://doi.org/10.1038/nmat1310

[5] Hohenberg, P., & Kohn, W. (1964). Inhomogeneous electron gas. Physical Review, 136(3B), B864–B871. https://doi.org/10.1103/PhysRev.136.B864

[6] Kohn, W., & Sham, L. J. (1965). Self-consistent equations including exchange and correlation effects. Physical Review, 140(4A), A1133–A1138. https://doi.org/10.1103/PhysRev.140.A1133

[7] Perdew, J. P., Burke, K., & Ernzerhof, M. (1996). Generalized gradient approximation made simple. Physical Review Letters, 77, 3865–3868. https://doi.org/10.1103/PhysRevLett.77.3865

[8] Singh, D. J., & Nordström, L. (2006). Planewaves, pseudopotentials and the LAPW method. Springer. https://doi.org/10.1007/978-0-387-28780-5

Received: Aug 10, 2023

Volume 36 No. 4, 2023, 621-634
ISSN: 1311-1728 (printed version); ISSN: 1314-8060 (on-line version)

[9] Blaha, P., Schwarz, K., Madsen, G. K. H., Kvasnicka, D., & Luitz, J. (2001). WIEN2k: An augmented plane wave + local orbitals program for calculating crystal properties. Vienna University of Technology. https://doi.org/10.1016/S0927-0256(02)00347-8

[10] Monkhorst, H. J., & Pack, J. D. (1976). Special points for Brillouin-zone integrations. Physical Review B, 13, 5188–5192. https://doi.org/10.1103/PhysRevB.13.5188

[11] Kittel, C. (2005). Introduction to solid state physics (8th ed.). Wiley. https://doi.org/10.1002/9780470381940

[12] Murnaghan, F. D. (1944). The compressibility of media under extreme pressures. Proceedings of the National Academy of Sciences, 30(9), 244–247. https://doi.org/10.1073/pnas.30.9.244

[13] Perdew, J. P., Burke, K., & Ernzerhof, M. (1996). Generalized gradient approximation made simple. Physical Review Letters, 77, 3865–3868. https://doi.org/10.1103/PhysRevLett.77.3865

[14] Hohenberg, P., & Kohn, W. (1964). Inhomogeneous electron gas. Physical Review, 136(3B), B864–B871. https://doi.org/10.1103/PhysRev.136.B864

[15] Kohn, W., & Sham, L. J. (1965). Self-consistent equations including exchange and correlation effects. Physical Review, 140(4A), A1133–A1138. https://doi.org/10.1103/PhysRev.140.A1133

[16] Kresse, G., & Furthmüller, J. (1996). Efficient iterative schemes for ab initio total-energy calculations using a plane-wave basis set. Physical Review B, 54, 11169–11186. https://doi.org/10.1103/PhysRevB.54.11169

[17] Kresse, G., & Joubert, D. (1999). From ultrasoft pseudopotentials to the projector augmented-wave method. Physical Review B, 59, 1758–1775. https://doi.org/10.1103/PhysRevB.59.1758

[18] Anisimov, V. I., Zaanen, J., & Andersen, O. K. (1991). Band theory and Mott insulators: Hubbard U instead of Stoner I. Physical Review B, 44, 943–954. https://doi.org/10.1103/PhysRevB.44.943

[19] Shi, L. J., Duan, Y., & Qin, H. (2010). First-principles study of transition-metal-doped MgO. Physics Letters A, 374, 121–125. https://doi.org/10.1016/j.physleta.2010.01.020

[20] Errico, L. A., Rentería, M., & Weissmann, M. (2005). Magnetic properties of transition-metal-doped oxides. Physical Review B, 72, 184425. https://doi.org/10.1103/PhysRevB.72.184425

[21] Duhalde, S., Vignolo, M. F., Golmar, F., et al. (2005). Ferromagnetism in Cu-doped oxide semiconductors. Physical Review B, 72, 161313. https://doi.org/10.1103/PhysRevB.72.161313

Received: Aug 10, 2023